ELSEVIER

Chemical Engineering Journal 133 (2007) 283–291

Chemical Engineering Journal

www.elsevier.com/locate/cej

Modelling solubility of solid sulphur in natural gas

Pierre Cézac [a], Jean-Paul Serin [a,*], Jacques Mercadier [a], Gérard Mouton [b]

[a] *Laboratoire de Thermique, Energétique et Procédés, Ecole Nationale Supérieure en Génie des Technologies Industrielle, Université de Pau et des Pays de l'Adour, BP 7511, 64075 Pau Cedex, France*

[b] *Total Infrastructures Gaz France, Direction Opérations, Services Supports Techniques-Méthodes, 7 rue de la Linière, 64140 Billère, France*

Received 10 November 2006; received in revised form 7 February 2007; accepted 21 February 2007

Abstract

The purpose of this work is to propose a model able to estimate the solubility of sulphur in natural gas transmission and distribution networks. Thus, we developed a model to predict the equilibrium solubility of elemental sulphur in natural gas containing low amount of H_2S, at pressure and temperature ranges lower than those encountered in production conditions. We established a reactive flash model. The constitutive equations are classically the chemical and physical equilibriums and partial mass balances. We chose the Peng–Robinson equation of state to describe the phase behaviour coupled with the van der Waals one-fluid mixing rules with one binary interaction coefficient. This approach needed critical parameters for each component. We determined the set of critical parameters for S_8 specie from three thermodynamic intrinsic properties including the description of sulphur dissociation reactions. Binary interaction parameters between CH_4, CO_2, H_2S and sulphur are obtained by optimisation from binary and ternary solubility data. Comparisons with experimental values of solid sulphur solubility show that the model is able to describe the sulphur solubility in synthetic natural gases. The application of our model to different natural gases indicated that under transport conditions sulphur solubility is less than 0.005 mg per normal cubic meter.

Keywords: Reactive flash; Modelling; Solid–gas equilibrium; Natural gas; Sulphur

1. Introduction

For years, the problem of sulphur deposition has been a notorious phenomenon when producing natural gas that is at high pressure, at high temperature and with a high amount of hydrogen sulphide [1]. However, the occurrence of sulphur precipitation has also been described in natural gas transmission and distribution networks. Chesnoy and Pack [2] found a sulphur deposit in a nozzle placed in a line connected to a natural gas pipeline. Wilkes and Pareek [3] observed sulphur deposits near the control valves of a gas turbine. Pack [4] studied natural gas transportation and listed the most common places where this phenomenon occurs. These authors considered that the deposit could come from gaseous elemental sulphur, which could be dissolved in gas. A drop in pressure or/and temperature could cause the solid sulphur to precipitate. Five articles present in the literature tried to model sulphur solubility [5–9] under the conditions of production. The various models described in these articles used the Peng–Robinson equation of state [10]. Tomcej et al. [5] used experimental critical temperature and pressure of sulphur to describe sulphur behaviour. They used the experimental critical coordinates of sulphur, which correspond to the lighter molecules of sulphur, whereas, in experimental conditions the most abundant sulphur specie is S_8. Gu et al. [6] proposed empirical critical coordinates for the S_8 molecule. These parameters were determined indirectly from the regression of the vapour pressure at lower temperatures. These authors also modified the van der Waals mixing rules for the EOS parameter *b*: they added two adjusted parameters for the calculation of *b*. So, for each binary, they got three adjusted parameters: two for the EOS parameter *b* calculation and one for the EOS parameter *a* calculation to fit a maximum of seven experimental points [6]. Moreover, these three parameters depend on temperature, and their evolution is complex. Sun and Chen [9] used the same model. They measured the solubility of solid sulphur between 303.2 and 363.2 K with pressures ranging from 300 to 450 bar in seven mixtures composed of methane, carbon dioxide and hydrogen sulphide. The three binary interaction coefficients

* Corresponding author. Tel.: +33 5 59 40 78 14.
E-mail address: jean-paul.serin@univ-pau.fr (J.-P. Serin).

1385-8947/$ – see front matter © 2007 Elsevier B.V. All rights reserved.
doi:10.1016/j.cej.2007.02.014

Nomenclature

a	attractive parameter in cubic EOS ($m^3\ mol^{-1})^2$
b	covolume in cubic EOS ($m^3\ mol^{-1}$)
c_p	heat capacity ($J\ mol^{-1}\ K^{-1}$)
f	fugacity (Pa)
H	molar enthalpy ($J\ mol^{-1}$)
k_{ij}	binary interaction coefficient for the parameter a
K	equilibrium constant
n	number of moles (mol)
P	pressure (bar)
P°	standard pressure (1 bar)
P^a	atmospheric pressure (1.01325 bar)
R	ideal gas constant ($8.314\ J\ mol^{-1}\ K^{-1}$)
T	temperature (K)
v	molar volume ($m^3\ mol^{-1}$)
y	vapour composition
Z	compressibility factor

Greek letters

ν	stoichiometric coefficient
ξ	reaction extent ($mol\ s^{-1}$)
ϕ	fugacity coefficient
ω	acentric factor

Subscript

c	critical property
1	refers to the solvent
2	refers to the solute
i,j	components of mixture

Superscript

cal	calculated
exp	experimental
f	fusion property
GP	ideal gas state property
L	liquid property
res	residual property
S	solid property
sub	sublimation property
V	vapour property
$\circ$	standard state
*	pure state
α	relative to orthorhombic sulphur (solid form)
β	relative to monoclinic sulphur (solid form)

were adapted from the experimental data sets. Unlike Gu et al. [6], the three adjusted parameters are temperature-independent. However, possible sulphur dissociation reactions were not taken into account in the two last works. Karan et al. [7] and Heidemann et al. [8] regressed the values of Peng–Robinson EOS parameters a and b of the S_8 specie between 393.15 and 913.15 K from the vapour pressure, the saturated liquid volume, the saturated vapour volume and the heat of vaporization of pure sulphur. All experimental data are taken from Tuller [11]. Equilibrium reactions between the sulphur molecules, which constitute sulphur vapours, and reactions that lead to the formation of polysulphanes are considered. For the products (S_7 to S and H_2S_2 to H_2S_9), the EOS characteristic parameters a and b are calculated from the so-called "sources species" [12,13]. The covolume of S_8 is assumed to be constant and the parameter a_{S8} has a particular expression. Then, due to the temperature range used to determine a_{S8}, this model is particularly appropriate to describe liquid and vapour sulphur behaviour. However, possible polymerization of sulphur in liquid phase was not taken into account. Under natural gas transportation conditions, only two authors [3,4] tried to predict the values of solid sulphur solubility. They used two different process simulation packages and explained neither the equations nor the data used to obtain their predictions. Furthermore, chemical reactions did not seem to be considered.

Thus, the objective of this work is to propose a knowledge model likely to describe the vapour–solid equilibrium of sulphur in ranges of temperature, pressure and composition, which correspond to natural gas transportation conditions, while considering the possible reactions involving sulphur.

2. Model description

Our modelling approach is a reactive flash model. It is based on a thermodynamic description of the macroscopic physical–chemical phenomena occurring in a gas solid system, which is assumed perfectly mixed. Solid sulphur is supposed pure. Assuming the above conditions, unknown factors are the composition of the gaseous phase and possibly the quantity of solid sulphur.

2.1. Governing equations

2.1.1. Vapour–solid equilibrium of sulphur

The thermodynamic equilibrium conditions imply that pressure, temperature and fugacity are identical in both phases:

$$f_{S_8}^{*S}(T, P) = f_{S_8}^{V}(T, P, y) \tag{1}$$

where $f_{S_8}^{*S}$ is the fugacity of the pure solid specie S_8 at temperature T and pressure P; $f_{S_8}^{V}$ is the fugacity of S_8 in the vapour phase.

2.1.2. Gaseous chemical equilibriums

The chemical reactions are written:

$$\nu_1 A_1 + \nu_2 A_2 + \cdots \Leftrightarrow \nu_3 A_3 + \nu_4 A_4 + \cdots \tag{2}$$

where ν_i are stoichiometric coefficients.

The criterion of chemical reaction equilibrium is

$$\prod_i \left(\frac{f_i^V(T, P, y)}{P^\circ} \right)^{\nu_{i,r}} = K_r^\circ(T) \tag{3}$$

where Π_i signifies the product over all species i. P° is the standard pressure (1 bar) and K° is the standard state equilibrium constant.

We chose to consider two types of chemical equilibrium, namely formation of sulphur lighter molecules:

$$\frac{x}{8}S_8 \Leftrightarrow S_x, \quad x = 1, 7 \tag{4}$$

and formation of polysulfanes:

$$H_2S + \frac{x-1}{8} S_8 \Leftrightarrow H_2S_x, \quad x = 2, 9 \tag{5}$$

2.1.3. Partial mass balances

The partial mass balances are written as below:

$$n_i^S + n_i^V - n_i^A - \sum_r \nu_{i,r}\xi_r = 0 \tag{6}$$

where n_i^A is the number of moles for the specie i in the feed, ξ_r the extent of the reaction r and $\nu_{i,r}$ is the stoichiometric coefficient of the specie i in the reaction r.

2.1.4. Numerical procedure

The set of equations composes a non-linear system in which all the thermodynamic properties are expressed as function of composition, pressure and temperature (Table 1). The degree of freedom is null. The overall system is solved in steady state using the Newton–Raphson's method.

2.2. Thermodynamic models

2.2.1. Fugacities in the gaseous phase

We chose to use an equation of state to describe fugacity. This equation and mixing rules had to be selected. Harvey [14] studied the ability of a Virial EOS to model the solubility of a solid in supercritical fluids. He deduced that this type of equation was not suitable. Teja et al. [15], Schwarz and Nieuwoudt [16] and Nicolas et al. [17] compared cubic EOS (Soave Redlich and Kwong, Peng and Robinson or Patel Teja) with non-cubic EOS (SAFT, SPHC, Sanchez Lacombe or Lennard Jones type). In most of cases, the cubic EOS best represented the experimental data, so we selected the Peng–Robinson equation of state. To extend the use of an equation of state to mixtures, we had to select mixing rules. There are classically two kinds of mixing rules: the mixing rules that are derived from the original van der Waals mixing rules, and the activity coefficient-based mixing rules. We selected the van der Waals mixing rules. They can be written as follows:

$$a_m = \sum_i \sum_j y_i y_j \sqrt{a_i a_j}(1 - k_{ij}(T))$$

$$b_m = \sum_i \sum_i y_i y_j \left(\frac{b_i + b_j}{2}\right) \tag{7}$$

where a_i and b_i are the pure characteristic EOS parameters, k_{ij} is the binary interaction coefficient between the species i and j.

2.2.2. Solid phase fugacity

The fugacity of pure solid specie can be written in different ways. The most common way relates the solid fugacity to the vapour fugacity under sublimation pressure [18]. We called it "the gas way":

$$f^{*S}(T, P) = \phi^{*V}(T, P^{sub}(T), y) P^{sub}(T) \exp\left(\int_{P^{sub}}^{P} \frac{v^{*S}}{RT} \mathrm{d}P\right) \tag{8}$$

where ϕ^{*V} is the fugacity coefficient of the pure specie at the sublimation pressure P^{sub}; v^{*S} is the molar volume of the pure solid. The Poynting term is often simplified assuming that the solid molar volume is pressure- and temperature-independent. The main advantage of this expression is that only two physical properties are required: the solid molar volume and the sublimation pressure. However, inasmuch as little data are available to calculate the sublimation pressure, Antoine equation is often used to extrapolate it. All five of the authors who modelled sulphur solubility under production conditions [5–9] utilized this "gas way". Under 330 K, the sublimation pressure is unknown [19]. So, the "gas way" cannot be rigorously used to express solid sulphur fugacity under natural gas transportation conditions. Another approach to express the pure solid fugacity is to link it to the pure liquid fugacity [18]. We called it "the liquid way":

$$\ln\left(\frac{f^{*S}(T, P)}{f^{*L}(T, P)}\right) = -\frac{\Delta H^f(T^f, P)}{RT}\left(1 - \frac{T}{T^f}\right) - \frac{\Delta c_p^{L-S}(T^f, P)}{R}\left[1 - \ln\left(\frac{T^f}{T}\right) - \frac{T^f}{T}\right] \tag{9}$$

where ΔH^f is the fusion enthalpy; T^f the fusion temperature at pressure P; Δc_p^{L-S} is the difference between the heat capacities of the pure liquid and the pure solid. The last right-hand term is an approximation, because the difference in heat capacities is considered as a constant and is evaluated at the fusion temperature. Therefore, the accuracy of this approximation decreases when the temperature moves away from the fusion temperature, which poses a problem to describe gas solid systems at low temperatures such as in gas transportation conditions. So, we proposed a new thermodynamic path to obtain pure solid

Table 1
Variables and equations of the model

Unknown variables		Equations	
Solid amount	1	$n_i^S + n_i^V - n_i^A - \sum_r \nu_{i,r}\xi_r = 0$	nc
Reaction extents	r	$f_{S_8}^{*,S}(T, P) = f_{S_8}^{V}(T, P, y)$	1
Vapour composition	nc	$\prod_i \left(\frac{f_i^V(T,P,y)}{P^\circ}\right)^{\nu_{i,r}} = K_r^\circ(T)$	r
Total	$nc + r + 1$	Total	$nc + r + 1$

Table 2
Values and sources of the data needed to express solid fugacity

Property	Symbol	Value	References
Solid density (kg m^{-3})	ρ^{s}	2070 (orthorhombic), 1960 (monoclinic)	[26]
Saturation pressure (Pa)	P^{sat}		[19]
Liquid density (kg m^{-3})	ρ^{l}		[19]
Liquid heat capacity (J g^{-1} K^{-1})	cp^{l}		[27]
Solid heat capacities (J g^{-1} K^{-1})	cp^{α} and cp^{β}		[27]
Ideal gas state S_8 heat capacity (J mol^{-1} K^{-1})	cp^{GP}		[28,29]
Transition temperature (K)	T^{tr}	368.46	[27]
Heat of transition (kJ mol^{-1})	ΔH^{tr}	3.2	[27]
Fusion temperature (K)	$T^{f\beta}$	392.75	[27]
Heat of fusion (kJ mol^{-1})	$\Delta H^{f\beta}$	12.86	[27]
Vaporization enthalpy at fusion temperature (kJ mol^{-1})	ΔH^{V}	91	[11]

fugacity:

$$\ln\left(\frac{f^{*S}(T,P)}{f^{*L}(T^f,P^a)}\right) = -\left(\frac{\Delta H^f(T^f,P^a)+\Delta H^V(T^f,P^{sat}(T^f))-HC}{RT}\right)\times\left(1-\frac{T}{T^f}\right)-\int_{T^f}^{T}\frac{\int_{T^f}^{T}\Delta c_p^{*S-GP}(T,P^a)\,dT}{RT^2}\,dT + \frac{v^{*S}}{RT}(P-P^a) \quad (10)$$

where

$$HC = H^{res}(T^f,P^{sat}(T^f)) + \left(v^{*L}-T^f\left(\frac{\partial v^{*L}}{\partial T}\right)_{P^a}\right)(P^a-P^{sat}((T^f)) \quad (11)$$

A demonstration of this expression is given in the Appendix A.

P^a is the atmospheric pressure (1.01325 bar); P^{sat} the saturation pressure; GP refers to the ideal gas state; H^{res} the residual enthalpy; ΔH^v the vaporization enthalpy; v^L is the liquid molar volume. T^f, ΔH^f, Δc_p^{*S-GP}, v^{*S} are respectively the fusion temperature, the enthalpy of fusion, the difference between the heat capacities of ideal gas and pure solid, and molar solid volume of solid sulphur under atmospheric pressure. The fugacity of the pure liquid is calculated under atmospheric pressure, so the enthalpy of fusion and the solid heat capacities are necessary under this pressure. To correct the pressure, a Poynting term is used (the last right hand term). Moreover, according to the temperature range, the thermodynamic stable form of solid sulphur can be monoclinic (β-form) or orthorhombic (α-form). From the data of Tuller [11], the transition temperature of crystalline sulphur can be given as a function of pressure. So, we regressed a correlation between the transition pressure and the transition temperature to determine the stable form of solid sulphur. This expression is:

$$P^{tr} = 24.962(T^{tr}-273.15)-2380.3 \quad (12)$$

where P^{tr} is the transition pressure in bar, and T^{tr} is the transition temperature in Kelvin. This correlation provides a deviation in pressure of 3.8%.

If the β-form is the solid stable form, its fugacity is calculated according to Eq. (13). Fugacity of the α-form is given by:

$$\ln\frac{f^{*\alpha}(T,P^a)}{f^{*\beta}(T,P^a)} = -\frac{\Delta H^{tr}(T,P^a)}{R}\left(\frac{1}{T}-\frac{1}{T^{tr}}\right) - \int_{T^{tr}}^{T}\frac{\int_{T^{tr}}^{T}(c_p^{*\alpha}(T,P^a)-c_p^{*\beta}(T,P^a))\,dT}{RT^2}\,dT \quad (13)$$

A demonstration of this expression is given in the Appendix A.

The data sources required to express solid fugacity are reported in Table 2.

2.2.3. Chemical equilibrium constants

They only depend on temperature. They are directly linked to the standard free Gibbs energy. All the data except for H_2S_x are available in the databank of the National Institute of Standards Technology. We used for H_2S_x the data reported by Heidemann et al. [8]. Polynomial expressions of the chemical equilibrium constants are given in Table 3.

2.2.4. Parameters of the model

Calculations using the Peng–Robinson equation of state require the critical temperature, the critical pressure and the acentric factor of each compound. For all non-sulphured compounds of natural gas except hydrogen sulphide, these values are available in Chemistry Data Series. For polysulfanes H_2S_2 to H_2S_5, Simmrock et al. [20] provide values for critical temperature, critical pressure and boiling temperature under atmospheric pressure. The acentric factor can be directly deduced from these data. Table 4 summarises these critical parameters. The characteristic parameters of the other polysulfanes are calculated according to the Prausnitz and Heidemann approach [12,13].

Only Gu et al. [6] published critical parameters for S_8. They obtained these values by minimization between experimental and calculated vapour pressures. Moreover, they neglected the reactions of dissociation of sulphur in vapour phase. We chose to determine the S_8 critical parameters from three properties of pure sulphur: vapour pressure, liquid molar volume and vapour molar volume. Moreover, reactions leading to the formation of S_7 to S from S_8 are considered. So, estimation of the S_8

Table 3
Temperature dependence of the equilibrium constants [8]

Reaction product	A	B	C	D
H_2S_2	8.7174E−01	−2.0044E−03	1.5149E−06	−1.3934E+03
H_2S_3	−1.8627E+00	1.3053E−03	−6.8075E−07	−1.2789E+03
H_2S_4	−4.5911E+00	4.5883E−03	−2.8467E−06	−1.0545E+03
H_2S_5	−7.3191E+00	7.8764E−03	−5.0187E−06	−7.6415E+02
H_2S_6	−1.0122E+01	1.1350E−02	−7.3381E−06	−4.4379E+02
H_2S_7	−1.2789E+01	1.4484E−02	−9.3892E−06	5.6411E+01
H_2S_8	−1.5509E+01	1.7752E−02	−1.1545E−05	6.9474E+02
H_2S_9	−1.8258E+01	2.1097E−02	−1.3770E−05	1.3589E+03
S_1	5.4733E+01	−2.3420E−02	2.4206E−05	−1.1118E+05
S_2	2.8568E+01	−7.9226E−03	5.1425E−06	−2.2057E+04
S_3	1.7790E+01	−5.8859E−03	3.1369E−06	−1.4827E+04
S_4	1.1252E+01	−2.5687E−03	1.1078E−06	−1.0155E+04
S_5	3.6273E+00	−3.7454E−04	−3.1316E−07	−3.9490E+03
S_6	2.7090E+00	−1.1796E−03	6.5280E−07	−1.9217E+03
S_7	2.0176E+00	−3.9211E−04	2.2272E−07	−1.5594E+03

$\mathrm{Log}_{10}(K^{\circ}(T)) = A + BT + CT^2 + (D/T)$, Temperature range: 200 to 600 K.

acentric factor and critical temperature and pressure is obtained by minimization of the following objective function:

$$f^{\mathrm{obj}} = \sum_{i=1}^{3} \sqrt{\frac{1}{\mathrm{np\ exp}(i)} \sum_{j=1}^{\mathrm{np\ exp}(i)} \left(\frac{y_{i,j}^{\mathrm{exp}} - y_{i,j}^{\mathrm{cal}}}{y_{i,j}^{\mathrm{exp}}} \right)^2} \quad (14)$$

where i indicates the given property (1: saturation pressure; 2: vapour volume; 3 liquid volume), y^{exp} and y^{cal} are respectively the experimental value of sulphur and the value estimated by means of the model. np exp(i) is the number of experimental points available for the property i. Experimental data needed are proposed by West and Menzies [21] and Tuller [11]. The characteristic parameters of the other sulphur species (S_x) are calculated according to the Prausnitz and Heidemann approach [12,13].

We obtained the following values: $T_c = 1065$ K, $P_c = 52$ bar, and $\omega = 0.3805$. The relative root mean square deviations

$$\mathrm{RRMSD}(\%) = 100 \sqrt{\frac{1}{\mathrm{np\ exp}(i)} \sum_{j=1}^{\mathrm{np\ exp}(i)} \left(\frac{y_{i,j}^{\mathrm{exp}} - y_{i,j}^{\mathrm{cal}}}{y_{i,j}^{\mathrm{exp}}} \right)^2} \quad (15)$$

are respectively 2.4, 0.2, and 1.67% for the saturation pressure, liquid density and vapour density.

2.2.5. Binary interaction coefficients

For all non-sulphured compounds except hydrogen sulphide, the binary interaction coefficients are classically available in databank [22].

Table 4
Polysulphanes critical parameters [20]

	Critical temperature (K)	Critical pressure (bar)	Acentric factor
H_2S_2	572	59.9	0.139
H_2S_3	738	52	0.1
H_2S_4	855	44.3	0.059
H_2S_5	930	39.4	0.031

The knowledge of all binary interaction parameters between sulphur and other components should lead to a better description of the natural gas systems. Due to the lack of experimental data, we regressed the binary coefficients between sulphur and respectively CH_4, CO_2 and H_2S from sulphur solubility data in each binary. We assumed the other binary interaction coefficients to be equal to zero. Taking account of binary interactions between sulphur and three of the major natural gas components should allow us to describe natural gas systems with a good accuracy.

Solid sulphur solubility has been measured in pure gas by several authors. Table 5 lists the solvent and the operating conditions of the measurements. These data are limited to three solvents: methane, carbon dioxide and hydrogen sulphide. Moreover, the data of Kennedy and Wieland [23] seem questionable [5,24], so we decided not to take them into account. Consequently, we have four isotherms for the solubility of S_8 in H_2S, two for CO_2 and only one for the CH_4. Thus, we chose to include experimental sulphur solubility in ternary system reported by Sun and Chen [9]. We regressed the values of the binary interaction coefficients between sulphur and methane, carbon dioxide

Table 5
Experimental solid sulphur solubility in pure gas

Solvent	Temperature (K)	Pressure range (bar)	np	References
H_2S	316.26	70.3–311.6	5	[24]
	338.71	68.9–413.7	6	[23]
	338.7	70.3–311.6	5	[24]
	363.2	118.3–362.1	6	[6]
	366.48	104.8–311.6	4	[24]
CO_2	338.71	68.9–413.7	6	[23]
	363.2	120.7–405.2	7	[6]
	366.48	68.9–413.7	6	[23]
	383.2	158.6–386.2	5	[6]
CH_4	338.71	68.9–413.7	6	[23]
	366.48	68.9–413.7	6	[23]
	383.2	205.2–501.7	4	[6]

np is the number of experiments at the temperature indicated in the second column.

Table 6
Determined binary interaction coefficients

j	$k_{S_8,j}(T)$
CH_4	1.154–377/T
CO_2	0.2423–21.44/T
H_2S	0.093–2.079/T

or hydrogen sulphide by least squares minimization method. The evolution of these three binary interaction coefficients is presented in Table 6.

3. Results

3.1. Sulphur solubility in gas mixtures

We applied our model to solid sulphur solubility in four gas mixtures. Then we compared the solubility we calculated with experimental solubility obtained by Brunner and Woll [25]. Results are presented in Fig. 1. Predicted values agree with the measurements. Thus, for mixture 1, poor in H_2S, the deviation calculated by Eq. (16) is equal to 5.7%. It is maximum for mixture 2 with 22.3% and respectively 21.3% and 11.6% for mixtures 3 and 4.

$$\Delta_{S_8}(\%) = 100\sqrt{\frac{1}{\text{np exp}}\sum_{i=1}^{\text{np exp}}\left(\frac{y_{S_8 i}^{\text{exp}} - y_{S_8 i}^{\text{cal}}}{y_{S_8 i}^{\text{exp}}}\right)^2} \quad (16)$$

where y^{exp} and y^{cal} are respectively the experimental solubility of sulphur and the solubility estimated using the model. np exp is the number of experimental points available for each solubility isotherm.

The model makes it possible to describe the evolution of the solubility of solid sulphur in gas mixtures close to natural gas according to the temperature and the pressure. Mixture 1 is the closest to natural gases transported by the gas companies. It is also the one with the smallest difference between experimental and calculated solubility. The established model seems to be a correct tool for studying the solubility of solid sulphur in natural gas under the transport conditions.

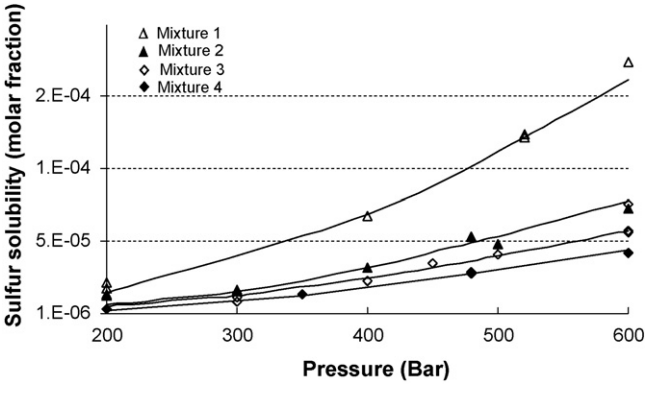

Fig. 1. Comparison between calculated (this work) and experimental solid sulphur solubility at 373.15 K [19].

Table 7
Comparison of predicted sulphur solubility (ppmv) (of this work) with Wilkes and Pareek [3] or with Pack [4] values

Temperature (°C)	Pressure (kPa)	Values proposed by [3] or [4]	Predicted values (this work)
42.8	3972	0.032 [3]	0.028
48.9	3972	0.051 [3]	0.052
47.0	8000	0.100 [4]	0.178
17.5	2000	0.001 [4]	0.001
41.2	6600	0.050 [4]	0.064
50.1	2000	0.030 [4]	0.0518

3.2. Sulphur solubility under gas transportation conditions

3.2.1. Comparison with previous models [3,4]

Only two authors [3,4] estimated sulphur solubility under these conditions. They used process simulation packages. Table 7 presents the comparison between the results of these works with our predicted values obtained using temperature, pressure and composition indicated in [3] and [4]. Deviation calculations show that our results are closer to those calculated by Wilkes and Pareek [3] than to those calculated by Pack [4]. The greater deviation with [3] is 14%, whereas, it reaches 44% with [4]. Due to the lack of experimental data, it is difficult to prove which values are the most accurate. In these both previous works the authors did not describe the thermodynamic model selected, the corresponding parameters, and nor the chemical reactions used. Furthermore, no comparison was made between calculated and available experimental values like those of Brunner and Woll [25]. Qualitatively two points should be noted: even if the deviation is important, the solubility values are generally in the same range of order and the solubility evolution with temperature is similar. The sulphur solubility increases with temperature.

3.2.2. Isosolubility of solid sulphur

We plotted isosolubility curves of solid sulphur for pure methane and three mixtures (Figs. 2–4). Temperature and pressure ranges correspond to those found in standard transport gas networks. The composition of the gases we studied is reported in Table 8. Gas B and gas H are two typical gas models used by gas transport companies. Gas B contains a great amount of nitrogen and has a lower heat capacity than gas H. Small amounts of

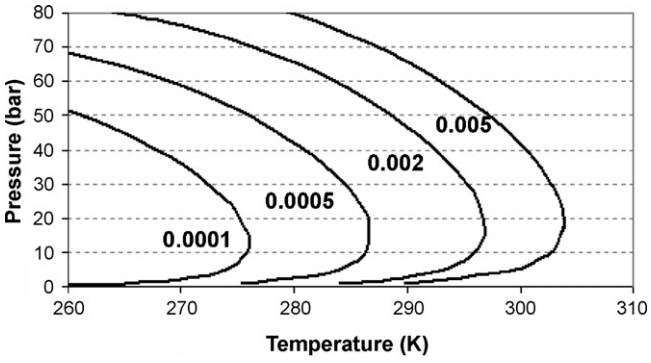

Fig. 2. Isosolubility (mg N m^{-3}) curves of sulphur in methane.

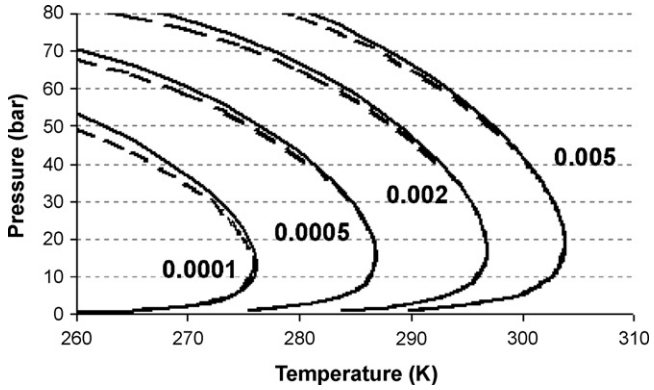

Fig. 3. Isosolubility curves of sulphur in the gas B (lines) and in the gas H (dashed lines).

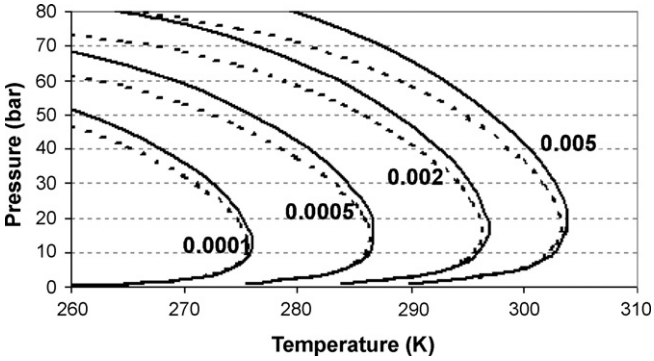

Fig. 4. Isosolubility curves of sulphur in methane (lines) and in GNL composition type (dashed lines).

heavier compounds are present in both gases. The composition of the last mixture is that of a liquefied natural gas. Due to the pressure and temperature ranges studied, in all cases, the solid sulphur is in the orthorhombic form. So, using the minimization method, we determined at fixed pressure the temperature at which the solubility is reached. The results are expressed in terms of sulphur in milligrams per normal cubic meter (0.005, 0.002, 0.0005 and 0.0001 mg N m^{-3}).

The isosolubility curves show the same tendency. From ranges of pressure from 5 to 40 bar, sulphur solubility is mainly dependent on temperature. Indeed, at approximately 20 bar, the curves has a vertical tangent. The higher the pressure, the more dependent on pressure the solubility is. The calculated solubility of sulphur in the gas considered is generally very low: less than 0.005 mg N m^{-3} (Fig. 2). Natural gas usually contains less than 3% of carbon dioxide. The presence of carbon dioxide does not seem to have a great influence. The calculated isosolubility curves for gases H and B were fairly identical to those in methane alone (Fig. 3). Fig. 4 permits to compare the sulphur isosolubility curves in methane and in a liquefied natural gas composition type. This type of natural gas contains more than 7% of ethane and no hydrocarbons greater than C4. The effect of ethane is observed at a pressure greater than 15 bar. The difference in solubility increases with pressure and temperature. The presence of ethane seems to improve the solubility of sulphur. Several authors [2–4] noted that a deposit of solid sulphur generally appears after a machine carries out a drop in pressure. Due to the Joule–Thomson effect, a pressure reduction causes a temperature reduction. Our results show that a fall in pressure and/or temperature involves a fall in solubility. Consequently, the natural gas can become oversaturated in sulphur and the excess of sulphur goes into a solid phase.

Table 8
Molar compositions (%) of the studied gas mixtures

	Gas B nitrogen rich gas	Gas H	Liquefied natural gas (LNG)
CH_4	83.9	98.1	90.69
C_2H_6	3.62	0.64	7.88
C_3H_8	0.74	0.21	0.82
C_4H_{10}	0.24	0.07	0.12
C_5H_{12}	0.14	0.03	
N_2	10.1	0.84	0.49
CO_2	1.24	0.11	

4. Conclusion

For several years, cases of sulphur deposition have been reported in the equipment of natural gas transmission systems. The purpose of this work is to propose a model able to estimate the solubility of sulphur under natural gas transportation conditions: low pressure, low temperature and low H_2S content. Thus, we established a reactive flash model. The constitutive equations are classically the chemical and physical equilibriums and partial mass balances. The possible reactions involving sulphur are taken into account. We chose the Peng–Robinson equation of state to describe the phase behaviour. Mixing rules are conventional: quadratic for a and linear for b with one binary interaction coefficient, which is temperature-dependent. This approach needed critical parameters for each component. We determined the set of critical parameters for S_8 specie from three thermodynamic intrinsic properties including the description of sulphur dissociation reactions. Binary interaction parameters between CH_4, CO_2, H_2S and sulphur are obtained by optimisation from binary and ternary solubility data. Comparison with experimental values of solid sulphur solubility shows that the model is able to describe the sulphur solubility in quaternary systems. Finally we established solid sulphur isosolubility curves for several gases. The curves show the same tendency. From ranges of pressure from 5 to 40 bar, sulphur solubility is mainly dependent on temperature. Indeed, at approximately 20 bar, the curves have a vertical tangent. The higher the pressure, the more dependent on pressure the solubility is. In the ranges of pressure, temperature and composition of the gas transportation conditions, the solubility of sulphur is very low. It is generally less than to 0.005 mg per normal cubic meter.

Appendix A. Appendix A

The expression of the molar Gibbs energy and its differential is for a pure compound:

$$G^* = H^* - TS^* \quad \text{(A.1)}$$

$$\mathrm{d}G = -\mathrm{S}^* \,\mathrm{d}T + v^* \,\mathrm{d}P \tag{A.2}$$

These relationships lead to:

$$\mathrm{d}\left(\frac{G^*}{RT}\right) = \frac{v^*}{RT}\,\mathrm{d}P - \frac{H^*}{RT^2}\,\mathrm{d}T \tag{A.3}$$

The potential of the pure compound is expressed from the ideal gas state potential.

$$\mu^*(T, P) = \mu^{0,\mathrm{GP}}(T) + RT\,\ln\left(\frac{f^*}{P^\circ}\right) \tag{A.4}$$

Considering a pure compound, the potential and the Gibbs energy are equal. So, using the relation (A.3) and (A.4), we obtain:

$$\mathrm{d}\,\ln\,f^* = \frac{v^*}{RT}\,\mathrm{d}P - \left(\frac{H^* - H^{\mathrm{GP}}}{RT^2}\right)\mathrm{d}T \tag{A.5}$$

This relationship is integrated at constant pressure (atmospheric pressure). The fusion temperature under atmospheric pressure is chosen as reference for the integration.

$$\ln\,\frac{f^{*\mathrm{S}}(T, P^{\mathrm{a}})}{f^{*\mathrm{S}}(T^f, P^{\mathrm{a}})} = \left(\frac{H^{*\mathrm{S}}(T^f, P^{\mathrm{a}}) - H^{\mathrm{GP}}(T^f)}{R}\right)\left(\frac{1}{T} - \frac{1}{T^f}\right) - \int_{T^f}^{T} \frac{\int_{t^f}^{T}(c_p^{*\mathrm{S}}(T, P^{\mathrm{a}}) - c_p^{\mathrm{GP}}(T))\,\mathrm{d}T}{RT^2}\,\mathrm{d}T \tag{A.6}$$

under atmospheric pressure, we also have the following relationships:

$$f^{*\mathrm{S}}(T^f, P^{\mathrm{a}}) = f^{*\mathrm{L}}(T^f, P^{\mathrm{a}}) \tag{A.7}$$

$$H^{*\mathrm{S}}(T^f, P^{\mathrm{a}}) = -\Delta H^f(T^f, P^{\mathrm{a}}) + H^{*\mathrm{L}}(T^f, P^{\mathrm{a}}) \tag{A.8}$$

Moreover, the liquid enthalpy can be expressed from the ideal gas state enthalpy according to:

$$H^{*\mathrm{L}}(T^f, P^{\mathrm{a}}) - H^{\mathrm{GP}}(T^f) = H^{\mathrm{res}}(T^f, P^{\mathrm{sat}}) - \Delta H^{\mathrm{V}}(T^f, P^{\mathrm{sat}}) + \left(v^{*\mathrm{L}} - T^f\left(\frac{\partial v^{*\mathrm{L}}}{\partial T}\right)_{P^{\mathrm{a}}}\right)(P^{\mathrm{a}} - P^{\mathrm{sat}}) \tag{A.9}$$

where the molar liquid volume is assumed to be pressure-independent.

Using the relationships (A.7)–(A.9), the expression of the pure solid fugacity (A.6) becomes:

$$\ln\left(\frac{f^{*\mathrm{S}}(T, P^{\mathrm{a}})}{f^{*\mathrm{L}}(T^f, P^{\mathrm{a}})}\right) = \left(\frac{-\Delta H^f(T^f, P^{\mathrm{a}}) + HC - \Delta H^{\mathrm{V}}(T^f, P^{\mathrm{sat}})}{R}\right) \times \left(\frac{1}{T} - \frac{1}{T^f}\right) - \int_{T^f}^{T} \frac{\int_{T^f}^{T}(c_p^{*\mathrm{S}}(T, P^{\mathrm{a}}) - c_p^{\mathrm{GP}}(T)\,\mathrm{d}T}{RT^2}\,\mathrm{d}T \tag{A.10}$$

where the constant HC is defined by:

$$\mathrm{HC} = H^{\mathrm{res}}(T^f, P^{\mathrm{sat}}) + \left(v^{*\mathrm{L}} - T^f\left(\frac{\partial v^{*\mathrm{L}}}{\partial T}\right)_{P^{\mathrm{a}}}\right) \times (P^{\mathrm{a}} - P^{\mathrm{sat}}) \tag{A.11}$$

To express the pure solid fugacity under another pressure, a Poynting term is added, which leads to:

$$\ln\left(\frac{f^{*\mathrm{S}}(T, P)}{f^{*\mathrm{L}}(T^f, P^{\mathrm{a}})}\right) = \left(\frac{-\Delta H^f(T^f, P^{\mathrm{a}}) + HC - \Delta H^{\mathrm{V}}(T^f, P^{\mathrm{sat}})}{R}\right)\left(\frac{1}{T} - \frac{1}{T^f}\right) - \int_{T^f}^{T} \frac{\int_{T^f}^{T}(c_p^{*\mathrm{S}}(T, P^{\mathrm{a}}) - c_p^{\mathrm{GP}}(T)\,\mathrm{d}T}{RT^2}\,\mathrm{d}T + \frac{v^{*\mathrm{S}}}{RT}(P - P^{\mathrm{a}}) \tag{A.12}$$

The Poynting term is simplified because the evolution of the solid molar volume with pressure and temperature is unknown. Thus, we supposed it independent of pressure and temperature.

In the case of sulphur, two thermodynamically stable solid forms exist: α- and β-forms. The β-form is the stable solid form at high temperatures. Its fugacity is calculated from the equation (A.12). According to the relation (A.5), for both forms and under atmospheric pressure, we can write:

$$\ln\,\frac{f^{*\alpha}(T, P^{\mathrm{a}})}{f^{*\alpha}(T^{\mathrm{tr}}, P^{\mathrm{a}})} = -\int_{T^{\mathrm{tr}}}^{\mathrm{T}}\left(\frac{H^{*\alpha}(T, P^{\mathrm{a}}) - H^{\mathrm{GP}}(T)}{RT^2}\right)\mathrm{d}T \tag{A.13}$$

$$\ln\,\frac{f^{*\beta}(T, P^{\mathrm{a}})}{f^{*\beta}(T^{\mathrm{tr}}, P^{\mathrm{a}})} = -\int_{T^{tr}}^{T}\left(\frac{H^{*\beta}(T, P^{\mathrm{a}}) - H^{\mathrm{GP}}(T)}{RT^2}\right)\mathrm{d}T \tag{A.14}$$

where T^{tr} is the transition temperature under atmospheric pressure.

At this temperature, the fugacity of the α-form is equal to the fugacity of the β-form. So, we deduced the following relationship:

$$\ln\,\frac{f^{*\alpha}(T, P^{\mathrm{a}})}{f^{*\beta}(T, P^{\mathrm{a}})} = -\int_{T^{\mathrm{tr}}}^{T}\left(\frac{H^{*\alpha}(T, P^{\mathrm{a}}) - H^{*\beta}(T, P^{\mathrm{a}})}{RT^2}\right)\mathrm{d}T \tag{A.15}$$

Finally:

$$\ln\,\frac{f^{*\alpha}(T, P^{\mathrm{a}})}{f^{*\beta}(T, P^{\mathrm{a}})} = -\frac{\Delta H^{\mathrm{tr}}(T^{\mathrm{tr}}, P^{\mathrm{a}})}{R}\left(\frac{1}{T} - \frac{1}{T^{\mathrm{tr}}}\right) - \int_{T^{\mathrm{tr}}}^{\mathrm{T}} \frac{\int_{T^{\mathrm{tr}}}^{T}(c_p^{*\alpha}(T, P^{\mathrm{a}}) - c_p^{*\beta}(T, P^{\mathrm{a}}))\,\mathrm{d}T}{RT^2}\,\mathrm{d}T \tag{A.16}$$

where ΔH^{tr} is the transition enthalpy under atmospheric pressure. A simplified Poynting term is added if the pressure is different from the atmospheric one.

References

[1] J.B. Hyne, Oil Gas J. (1968) 107–113.
[2] A.-B. Chesnoy, D.J. Pack, Oil Gas J. (1997) 74–78.
[3] C. Wilkes, V. Pareek, Energy-Tech Online (2001).
[4] D.J. Pack, Paper presented at the 14th Biennal Joint Technical Meeting on Pipelines Research, Berlin 2003, Paper no. 31, pp. 1–14.
[5] R.A. Tomcej, H. Kalra, B.E. Hunter, Paper presented at the 39th Annual Laurence Reid gas Conditioning Conference, Norman, Oklahoma, March 6–8, 1989, pp. 159–182.
[6] M.-X. Gu, Q. Li, S.-H. Zhou, W.-D. Chen, T.-M. Guo, Fluid Phase Equilib. 82 (1993) 173–182.
[7] K. Karan, R.A. Heidemann, L.A. Behie, Ind. Eng. Chem. Res. 37 (1998) 1679–1684.
[8] R.A. Heidemann, A.V. Phoenix, K. Karan, L.A. Behie, Ind. Eng. Chem. Res. 40 (2001) 2160–2167.
[9] C.-Y. Sun, G.-J. Chen, Fluid Phase Equilib. 214 (2003) 393–402.
[10] D.Y. Peng, D.B. Robinson, GPA Research Report, Tulsa, 1978.
[11] W.N. Tuller, The Sulphur Data Book, McGraw-Hill, New York, 1954.
[12] R.A. Heidemann, J.M. Prausnitz, Proc. Natl. Acad. Sci. U.S.A. 73 (1976) 1773–1776.
[13] R.A. Heidemann, J.M. Prausnitz, AIChE Annual Meeting, Chicago, 1976.
[14] A.H. Harvey, Fluid Phase Equilib. 130 (1997) 87–100.
[15] A. Teja, V. Smith, T. Sun, Fluid Phase Equilib. 150/151 (1998) 393–402.
[16] C. Schwarz, I. Nieuwoudt, J. Supercrit. Fluids 27 (2003) 133–144.
[17] C. Nicolas, E. Neau, S. Meradji, I. Raspo, Fluid Phase Equilib. 232 (2003) 219–229.
[18] J.M. Prausnitz, R.N. Lichtenthaler, E.G. de Azevedo, Molecular Thermodynamics of Fluid phase Equilibria, 2nd ed., Prentice-Hall, Englewood Cliffs, NJ, 1999.
[19] X. Shuai, A. Meisen, Oil Gas J. 93 (1995) 50–55.
[20] K. Simmrock, R. Janowsky R., A. Ohnsorge A., Critical Data of Pure Substances, Chemistry Data Series, Frankfurt/Main, 1986.
[21] W.A. West, A.W.C. Menzies, J. Chem. Phys. 33 (1929) 1880–1892.
[22] H. Knapp, R. Döring, L. Oellrich, U. Plöcker, J.M. Prausnitz, Vapour–Liquid Equilibria for mixtures of Low Boiling Substances, Chemistry Data Series, Frankfurt/Main, 1982.
[23] H.T. Kennedy, D.R. Wieland, Petroleum Transactions, AIME 219 (1960) 166–169.
[24] J.J. Roof, Soc. Pet. Eng. J. 11 (1971) 272–276.
[25] E. Brunner, W. Woll, Soc. Pet. Eng. J. 20 (1980) 377–384.
[26] K. Raznjevic, Tables et diagrammes thermodynamiques, Eyrolles, Paris, 1970.
[27] J. Chao, Hydrocarbon Proc. (1980).
[28] M.W. Chase, Jr., NIST-JANAF Thermochemical Tables, 4th ed., J. Phys. Chem. Ref. Data. Monogr. 9 (1998) 1–1951.
[29] O. Knacke, O. Kubaschewski, K. Hesselmann, Thermochemical Properties of Inorganic Substances II, 2nd ed., Springer-Verlag, Berlin, 1991.